J Therm Anal Calorim (2017) 129:801–808
DOI 10.1007/s10973-017-6234-3

Isothermal and nonisothermal crystallization kinetics of novel biobased poly(ethylene succinate-*co*-ethylene sebacate) copolymers from the amorphous state

Shoutian Qiu[1] · Zhiqiang Su[1] · Zhaobin Qiu[1]

Received: 14 December 2016 / Accepted: 22 February 2017 / Published online: 2 March 2017

Abstract In this work, the isothermal and nonisothermal crystallization kinetics of three novel biobased poly (ethylene succinate-*co*-ethylene sebacate) (PESSe) copolymers was systematically investigated with differential scanning calorimetry under different crystallization conditions from the amorphous state. For the isothermal cold crystallization kinetics study, the Avrami equation could well describe the crystallization process of PESSe at various crystallization temperatures. All three PESSe copolymers crystallized through the same crystallization mechanism; moreover, the overall isothermal cold crystallization rate of PESSe decreased with increasing ethylene sebacate (ESe) comonomer content. The nonisothermal cold crystallization kinetics of PESSe was also studied at different heating rates. With increasing ESe content or heating rate, the nonisothermal cold crystallization exotherm of PESSe copolymers shifted to high temperature range. Both the crystallization rate parameter and crystallization rate coefficient of PESSe copolymers decreased with increasing ESe content, indicating that PESSe copolymer with higher ESe content crystallized more slowly than that with lower ESe content. The Ozawa equation was used to analyze the nonisothermal cold crystallization kinetics of PESSe copolymers, which was found to fit the crystallization process very well.

✉ Zhaobin Qiu
qiuzb@mail.buct.edu.cn

[1] State Key Laboratory of Chemical Resource Engineering, MOE Key Laboratory of Carbon Fiber and Functional Polymers, Beijing University of Chemical Technology, Beijing 100029, China

Keywords Crystallization kinetics · Copolymers · DSC · Amorphous

Introduction

Biodegradable polymers have received more and more research interests because of their advantages in solving problems associated with both the fossil shortage and the environmental pollution [1–3]. Poly(ethylene succinate) (PES), a typical biodegradable polymer, has been widely studied in recent years, as it shows the comparative properties with traditional plastics such as polyethylene and polypropylene; moreover, the monomer for the synthesis of PES can also be prepared from renewable resources [4–13].

PES is a biodegradable polymer with its melting points over 100 °C and relatively good mechanical properties; therefore, PES may find many end uses as packing material and agricultural film in practical application fields. Despite its relatively high melting point and excellent mechanical properties, PES has not received more interests than some other commercially available biodegradable polyesters, such as poly(butylene succinate) (PBS) and poly(lactide) (PLA). To extend the application fields of PES, many efforts have been devoted to improving the physical properties. Copolymerization is one of the most effective methods in polymeric materials modification. As far as PES is concerned, some comonomers, such as adipic acid, butanediol, 1,8-octanediol, and 1,10-decanediol, have been used for the synthesis of PES-based copolymers to modify its chemical structure and adjust its physical properties [14–19]. We once synthesized a series of novel biobased poly(ethylene succinate-*co*-ethylene sebacate) (PESSe) copolyesters and studied their basic thermal properties, crystal structure, mechanical properties, and hydrolytic degradation behavior in detail [19]. PESSe

copolymers showed good mechanical properties, making them good candidates as packaging materials or to modify and improve the physical properties of other polymeric materials with poor properties through polymer blending; moreover, depending on ESe content, the mechanical properties may be adjusted to meet practical requirements. In addition, by adjusting ESe content, PESSe copolymers may show different thermal properties, mechanical properties, and hydrolytic degradation behaviors.

The crystallization kinetics study is of great interest and importance from both research and practical application viewpoints, as the final crystallinity as well as the crystalline structure and morphology not only affect the physical properties but also influence the biodegradation process of biodegradable polymers; moreover, such study is also related to polymer processing conditions. Depending on the initial state of the occurrence of crystallization, polymer crystallization may involve mainly two kinds of types, including melt crystallization from the crystal-free melt and cold crystallization from the completely amorphous state. In most cases, semicrystalline polymers usually only undergo melt crystallization, as they crystallize so fast that completely amorphous state cannot be achieved even fast cooling rate is used. Consequently, relative to polymer melt crystallization, polymer cold crystallization has seldom been reported [20–26]. As PESSe copolymers crystallize slowly, they can reach the completely amorphous state during fast cooling process from the crystal-free melt; therefore, they are good models to perform the polymer cold crystallization study. In this work, the cold crystallization kinetics study of PESSe copolymers was studied from the amorphous state in detail under different crystallization conditions, including both isothermal cold crystallization at different crystallization temperatures and nonisothermal cold crystallization at different heating rates. The novelty of this work may be summarized as follows. First, the effects of both different crystallization conditions and ESe content on the cold crystallization kinetics of novel PESSe copolymers were systematically investigated with DSC for the first time. Second, to our knowledge, this work may probably be the first systematic research to study the effect of comonomer content on the cold crystallization kinetics of biodegradable copolymers; therefore, it may provide a good example on how to perform the related study of other biodegradable polymeric materials based on copolymers.

Experimental

Materials

Three PESSe copolymers with different ESe contents of 5, 10, and 15% were synthesized in our lab as described elsewhere [19], and they were named as PESSe5, PESSe10, and PESSe15, respectively, for brevity. The weight average molecular weights were 8.7×10^4, 7.8×10^4, and 9.4×10^4 g mol^{-1} for PESSe5, PESSe10, and PESSe15, respectively.

Characterizations

The isothermal and nonisothermal cold crystallization behaviors of PESSe copolymers were systematically investigated with a TA instrument differential scanning calorimeter (DSC) Q100 under different crystallization conditions with a nitrogen flow of 50 mL min^{-1}. Before each DSC test, a fresh sample of about 5 mg was used. Through the following thermal treatment, the completely amorphous state of each sample was reached by heating at 20 °C min^{-1} to 140 °C, holding there for 3 min to erase any previous thermal history, and quenching to −80 °C at 60 °C min^{-1}. For the isothermal cold crystallization kinetics study, the sample was heated quickly from the amorphous state to desired crystallization temperature (T_c) and held for sufficient time to ensure complete crystallization. For the nonisothermal cold crystallization behavior study, the sample was heated from the amorphous state at different heating rates ranging from 4 to 10 °C min^{-1}.

Results and discussion

The isothermal cold crystallization kinetics studies of PESSe copolymers were first investigated at different T_c values of 20, 25, 30, and 35 °C in this work. The plots of relative crystallinity versus crystallization time for the three PESSe copolymers during isothermal cold crystallization process are shown in Fig. 1. From Fig. 1, the time required for each sample to complete crystallization became shorter with increasing T_c, while the time became longer with increasing ESe content at a given T_c. For example, at a T_c of 35 °C, it needed about 13 min for PESSe5 while about 17 and 30 min for PESSe10 and PESSe15, respectively, to complete crystallization, indicating that increasing ESe content decreased the isothermal cold crystallization of PESSe copolymers.

To better investigate the isothermal cold crystallization kinetics of PESSe copolymers, the well-known Avrami equation was used to analyze the related crystallization process. The Avrami equation describes the evolution of relative crystallinity (X_t) with crystallization time (t) as follows:

$$1 - X_t = \exp\left(-kt^n\right) \quad (1)$$

where n is the Avrami exponent, reflecting crystallization mechanism, and k is the crystallization rate constant,

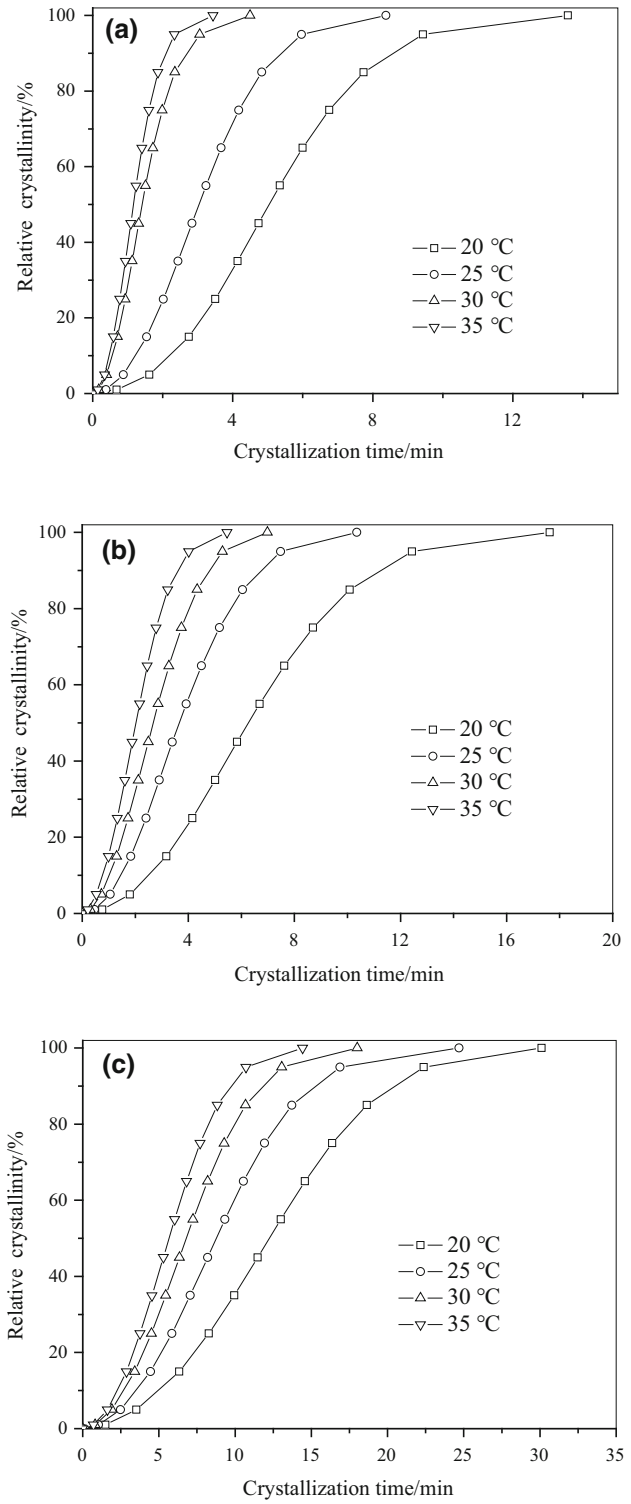

Fig. 1 Plots of relative crystallinity versus crystallization time for **a** PESSe5, **b** PESSe10, and **c** PESSe15 during isothermal cold isothermal crystallization

involving both nucleation and crystal growth [27, 28]. Figure 2 shows the corresponding Avrami plots of PESSe copolymers at indicated T_c values, from which a set of almost parallel lines were obtained for each copolyester. Therefore, the Avrami equation was suitable to fit the isothermal cold crystallization process of each copolyester.

From the plots shown in Fig. 2, the Avrami parameters of n and k were acquired and are listed in Table 1 for comparison. Table 1 clearly shows that the n values varied slightly between 2.0 and 2.2 for the three PESSe copolymers after crystallizing at indicated T_c values, indicating that PESSe copolymers should crystallize through the same crystallization mechanism [29]. The k values are also summarized in Table 1; moreover, the k values were greater at higher T_c than at lower T_c for each copolyester when the n values were the same. As the unit of k was ($\min^{-n}$), it was not reasonable to use the k values to directly compare the crystallization rate of different samples at different T_c values, if the n values were not the same. Thus, crystallization half-time ($t_{0.5}$), the time required to achieve 50% of the final crystallinity, was used to compare the crystallization rate, which could be calculated through the following equation:

$$t_{0.5} = \left(\frac{\ln 2}{k}\right)^{1/n} \tag{2}$$

Accordingly, the reciprocal of $t_{0.5}$ may represent the crystallization rate. Figure 3 shows the temperature dependence of $t_{0.5}$ for PESSe copolymers at indicated T_c values. From Fig. 3, $t_{0.5}$ decreased with increasing T_c for each sample, indicating faster crystallization rate at higher T_c. The increased isothermal cold crystallization rate with increasing T_c of PESSe copolymers was similar to that of their homopolymer PES undergoing isothermal cold crystallization process [11]. On the other hand, $t_{0.5}$ increased significantly with increasing ESe content for the three PESSe copolymers at a given T_c, suggesting that increasing the comonomer content decreased obviously the isothermal cold crystallization rate of PESSe.

In the above section, the isothermal cold crystallization kinetics of PESSe copolymers was studied with DSC at indicated T_c values and analyzed by the well-known Avrami equation. In this section, the nonisothermal cold crystallization behavior of PESSe copolymers was further investigated with DSC at different heating rates. The effects of different heating rates and ESe content on the nonisothermal cold crystallization behavior of PESSe copolymers were studied with DSC in detail. Figure 4a displays the nonisothermal cold crystallization behavior of PESSe5 at indicated heating rates to study the effect of heating rate, while Fig. 4b illustrates the nonisothermal cold crystallization behavior of PES and PESSe copolymers at the same heating rate of 6 °C $\min^{-1}$ to investigate the influence of ESe content. Figure 4a shows that the nonisothermal cold crystallization exotherm of PESSe5

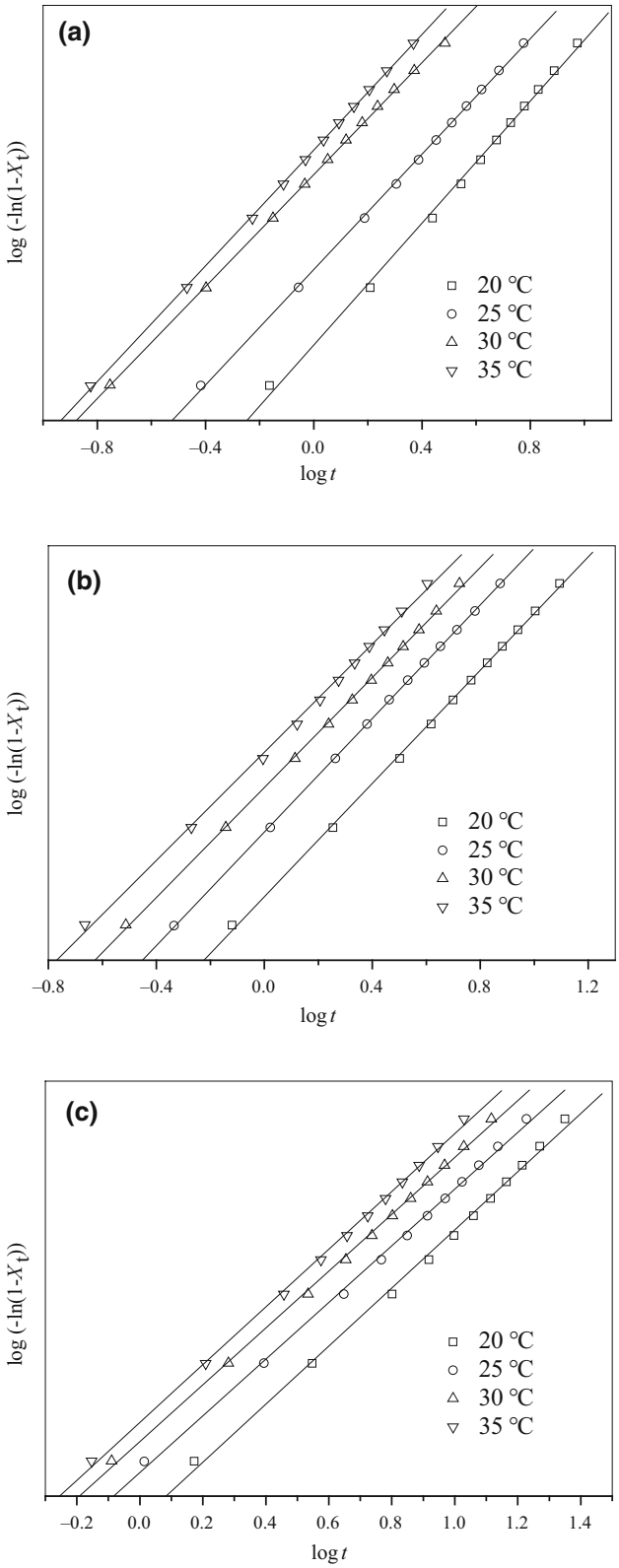

Fig. 2 Avrami plots of **a** PESSe5, **b** PESSe10, and **c** PESSe15 during isothermal cold crystallization

Table 1 Isothermal crystallization kinetics parameters based on the Avrami equation of PESSe copolymers from the amorphous state

Samples	T_c/°C	n	k/min^{-n}
PESSe5	20	2.2	1.97×10^{-2}
	25	2.1	6.91×10^{-2}
	30	2.0	3.36×10^{-1}
	35	2.1	5.05×10^{-1}
PESSe10	20	2.0	1.62×10^{-2}
	25	2.1	4.76×10^{-2}
	30	2.0	1.00×10^{-1}
	35	2.0	1.80×10^{-1}
PESSe15	20	2.1	3.75×10^{-3}
	25	2.0	8.32×10^{-3}
	30	2.1	1.39×10^{-2}
	35	2.1	1.92×10^{-2}

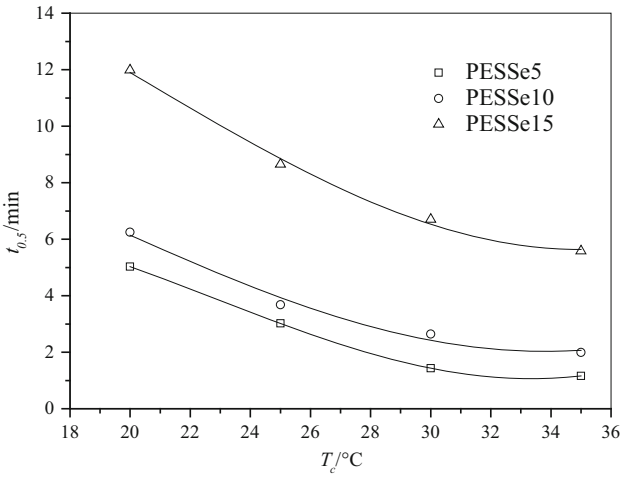

Fig. 3 T_c dependence of $t_{0.5}$ for the PESSe copolymers during isothermal crystallization process from the amorphous state

shifted upward to high temperature range with increasing heating rate, indicating the occurrence of nonisothermal cold crystallization at high crystallization temperature. With increasing heating rate from 4 to 10 °C min^{-1}, the nonisothermal cold crystallization peak temperature (T_p) of PESSe5 increased from 30.5 to 40.0 °C. Figure 4b demonstrates that the nonisothermal cold crystallization exotherm shifted to high temperature range with increasing ESe content, suggesting that the nonisothermal cold crystallization became more difficult for PESSe copolymer with high ESe content. With increasing ESe content from 5 to 15 mol%, T_p increased from 34.3 to 45.3 °C for PESSe copolymers. Moreover, the nonisothermal cold crystallization of PES was also included in Fig. 4b for

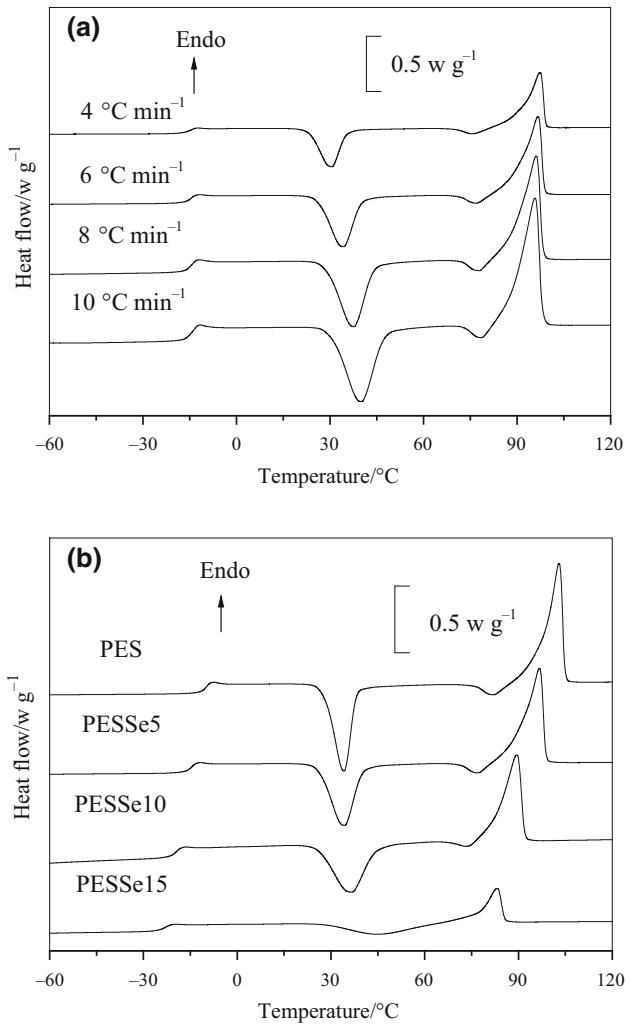

Fig. 4 DSC heating traces of **a** PESSe5 at indicated heating rates and **b** PESSe copolymers at a heating rate of 6 °C min^{-1} from the amorphous state

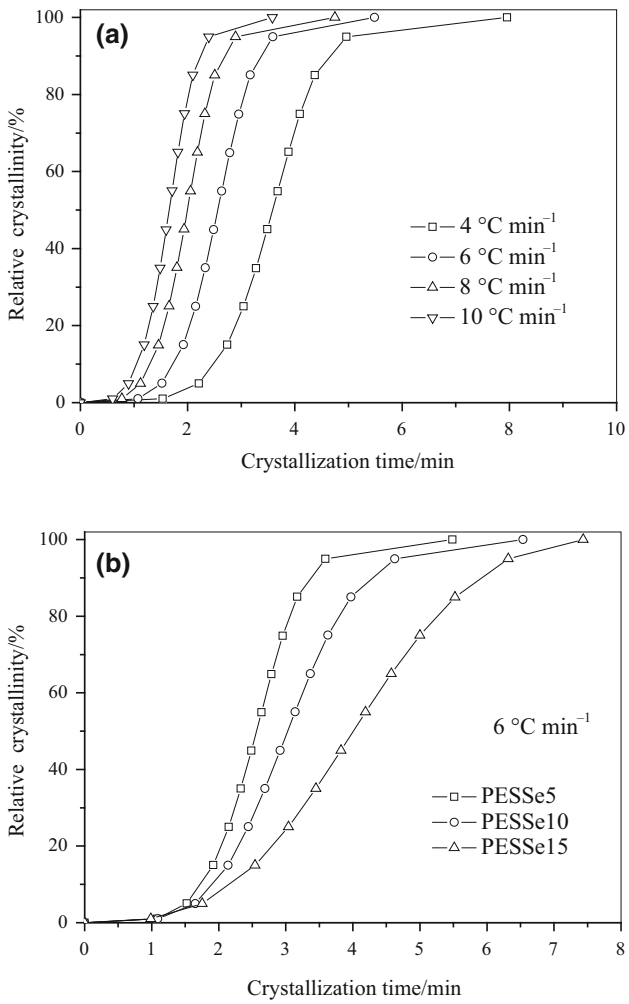

Fig. 5 Plots of relative crystallinity versus crystallization time for **a** PESSe5 at indicated heating rates and **b** PESSe copolymers at a heating rate of 6 °C min^{-1} from the amorphous state

comparison. The T_p value was 34.1 °C for PES, which was lower than those of all copolymers, further evidencing that the introduction of ESe retarded the nonisothermal cold crystallization process.

On the basis of Fig. 4 and the relationship between crystallization temperature and crystallization time, we could get the development of relative crystallinity with crystallization time for PESSe copolymers during nonisothermal cold crystallization. Figure 5a displays the plots of relative crystallinity versus crystallization time for PESSe at indicated heating rates, while Fig. 5b illustrates the evolution of relative crystallinity with crystallization time for PESSe with different ESe contents at the same heating rate of 6 °C min^{-1}. Figure 5 clearly shows that crystallization time became shorter with increasing heating rate for PESSe5, indicating faster nonisothermal cold crystallization rate at higher heating rate; moreover, crystallization time became longer with increasing ESe content for PESSe copolymers at the same heating rate, suggesting a slower crystallization rate for PESSe copolymer with higher ESe content. From Fig. 5, nonisothermal cold crystallization half-time ($t_{1/2}$), the time required to finish 50% of final crystallinity, was directly read from the plots of relative crystallinity versus crystallization time and the values are listed in Table 2. From the summary of $t_{1/2}$ listed in Table 2, we could draw the same conclusions as from Fig. 5. In brief, increasing heating rate or decreasing ESe content accelerated the nonisothermal cold crystallization of PESSe copolymers.

To better understand the influence of ESe content on the nonisothermal cold crystallization behavior, the crystallization rate parameter (CRP) and crystallization rate coefficient (CRC) of PESSe copolyesters were calculated in this research. In the literature, Zhang et al. introduced CRP to compare the crystallization rate of different

Table 2 Nonisothermal cold crystallization parameters of PESSe copolymers

Samples	Heating rate/°C min^{-1}	T_p/°C	$t_{1/2}$/min
PESSe5	4	30.5	3.61
	6	34.3	2.58
	8	37.6	2.01
	10	40.0	1.66
PESSe10	4	30.8	4.49
	6	36.6	3.08
	8	40.0	2.40
	10	42.3	2.04
PESSe15	4	39.0	5.63
	6	45.3	4.00
	8	49.1	3.02
	10	51.9	2.47

systems [30], which may be determined from the slope of the plot of $1/t_{1/2}$ versus cooling (or heating) rate. The greater CRP value indicates faster crystallization rate. Figure 6 illustrates the related plots of $1/t_{1/2}$ versus heating rate for PESSe copolyesters, from which the CRP values were calculated to be 5.4×10^{-2}, 4.5×10^{-2}, and 3.8×10^{-2} °C^{-1} for PESSe5, PESSe10, and PESSe15, respectively. Consequently, increasing ESe content decreased the nonisothermal cold crystallization rate of PESSe copolymers.

In the literature, Khanna once introduced CRC to rank the crystallization rate of different systems. CRC indicated a change in cooling rate required for 1 °C change in the supercooling of the polymer melt, which may be calculated from the slope of the plot of cooling rate versus $T_m - T_p$, where T_m and T_p are the melting point and nonisothermal melt crystallization peak temperature, respectively. Therefore, the greater CRC value indicated fast crystallization rate [31]. To better understand the nonisothermal crystallization behaviors of PESSe copolymers from the amorphous state, the CRC values were also estimated in this work. In this research, PESSe copolymers were nonisothermally crystallized from the completely amorphous state; therefore, $T_p - T_g$ (T_g is glass transition temperature) was used instead of $T_m - T_p$ to determine CRC, which should represent a change in heating rate required for 1 °C change in the superheating of the amorphous phase [22, 23]. Figure 7 shows the plots of heating rate versus $T_p - T_g$ for PESSe copolyesters, from which the CRC values were determined to be 0.62, 0.50, and 0.45 min^{-1} for PESSe5, PESSe10, and PESSe15, respectively. In brief, increasing ESe content decreased the nonisothermal cold crystallization rate of PESSe copolymers. From the above mentioned studies, both the CRP and CRC values decreased with increasing ESe content, indicating that PESSe copolymer with higher ESe content crystallized more slowly than that with lower ESe content during nonisothermal cold crystallization.

The nonisothermal cold crystallization kinetics of PESSe copolymers was analyzed by the recognized Ozawa equation. The Ozawa equation is described as follows:

$$X_T = 1 - \exp\left(\frac{-K(T)}{\Phi^m}\right) \quad (3)$$

where X_T is the relative crystallinity at T_c, Φ is cooling (or heating) rate, $K(T)$ is the cooling (or heating) function at T_c, and m is the Ozawa exponent reflecting the type of nucleation and growth mechanism [32]. For example, Fig. 8 shows the typical Ozawa plots of PESSe15 at indicated T_c values of 30, 32, 34, and 36 °C. The linear plots shown in Fig. 8 indicate that the Ozawa equation was

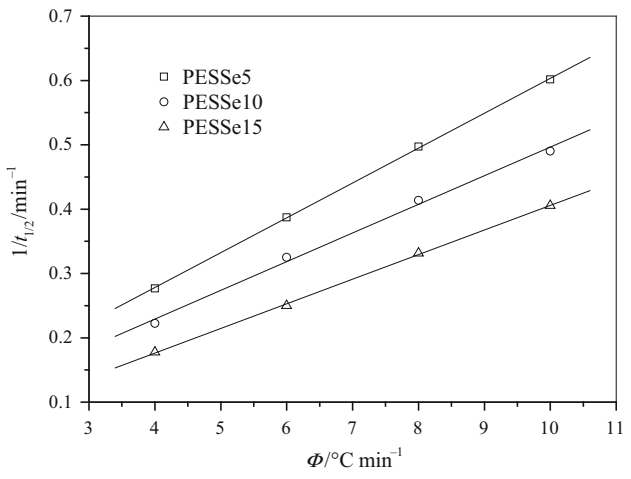

Fig. 6 Plots of $1/t_{1/2}$ versus heating rate for PESSe copolymers to determine the CRP values

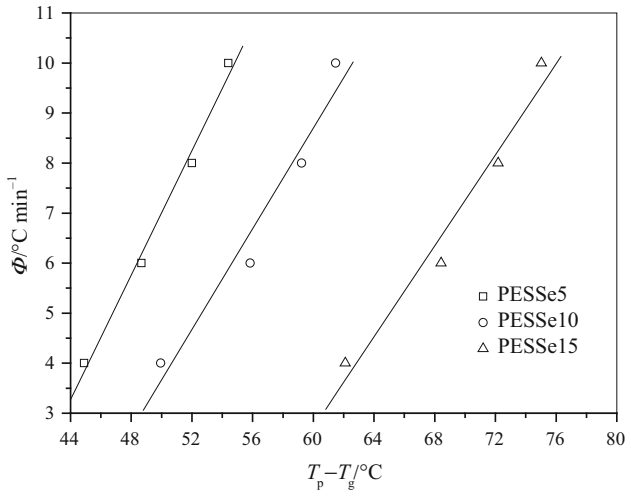

Fig. 7 The plots of heating rate versus $T_p - T_g$ for PESSe copolymers to estimate the CRC values

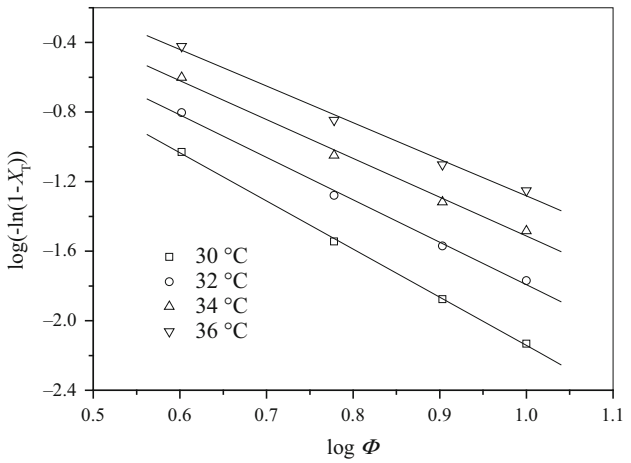

Fig. 8 The Ozawa plots of the PESSe15

Table 3 Nonisothermal crystallization kinetics parameters of the PESSe copolymers calculated from the Ozawa equation from the amorphous state

Samples	T_c/°C	m	$K(T)$/(°C min^{-1})^n
PESSe5	30	3.9	2.26
	32	3.7	2.41
	34	3.4	2.55
	36	3.2	2.62
PESSe10	30	3.6	2.00
	32	3.3	2.05
	34	3.1	2.13
	36	2.9	2.17
PESSe15	30	2.8	6.30×10^{-1}
	32	2.4	6.48×10^{-1}
	34	2.2	7.22×10^{-1}
	36	2.1	8.25×10^{-1}

suitable to describe the nonisothermal cold crystallization kinetics of PESSe5. In addition, PESSe5 and PESSe10 showed the similar results as PESSe5. For brevity, they were not shown here. In the literature, the Ozawa equation could fit the nonisothermal melt and cold crystallization kinetics of PES [11, 33] but failed to analyze the nonisothermal melt crystallization kinetics of PBS and poly (ethylene suberate) [33, 34]. Table 3 lists the obtained m and $K(T)$ values of PESSe copolymers. From Table 3, the following conclusions were drawn. First, the m values were not constant and changed with T_c and ESe content, indicating that the crystallization mechanism should also not be the same and varied. Second, $K(T)$ gradually increased with increasing T_c for each sample, suggesting faster crystallization rate at higher T_c. Such enhanced crystallization rate with increasing T_c was reasonable for semicrystalline polymers during nonisothermal cold crystallization from the amorphous state. The crystallizability of polymer is obviously improved at higher T_c than at lower T_c, as the mobility of polymer chain increases with increasing T_c, and the crystal growth should be dominant factor of influencing the overall crystallization rate.

Conclusions

In this research, the isothermal and nonisothermal cold crystallization kinetics of three novel biobased PESSe copolymers was studied for the first time with DSC under different crystallization conditions in detail. In the case of isothermal cold crystallization kinetics study, three PESSe copolymers with different ESe contents were isothermally crystallized at different crystallization temperatures ranging from 20 to 35 °C from the amorphous state. Through the Avrami equation analysis, the related isothermal cold crystallization kinetics data were obtained. Regardless of crystallization temperature and ESe content, PESSe copolymers crystallized through the same crystallization mechanism; however, increasing ESe content or decreasing crystallization temperature decreased the cold crystallization rate of PESSe copolymers. In the case of nonisothermal cold crystallization kinetics study, PESSe copolymers were nonisothermally crystallized at different heating rates ranging from 4 to 10 °C min^{-1} from the amorphous state. The nonisothermal cold crystallization exotherm of PESSe copolymers shifted upward to high temperature range with increasing heating rate or ESe content. Increasing ESe content reduced both the crystallization rate parameter and crystallization rate coefficient of PESSe copolymers, suggesting that PESSe copolymer with higher ESe content crystallized more slowly than that with lower ESe content. The Ozawa equation was found to be able to well fit the nonisothermal cold crystallization process of PESSe copolymers.

Acknowledgements The authors thank the National Natural Science Foundation, China (51373020, 51573016 and 51521062) for the support of this research.

References

1. Papageorgiou GZ, Bikiaris DN, Achilias DS, Papastergiadis E, Docoslis A. Crystallization and biodegradation of poly(butylene azelate): comparison with poly(ethylene azelate) and poly(propylene azelate). Thermochim Acta. 2011;515:13–23.
2. Zhou C, Wei Z, Yu Y, Wang Y, Li Y. Biobased copolyesters from renewable resources: synthesis and crystallization kinetics of poly(propylene sebacate-*co*-isosorbide sebacate). RSC Adv. 2015;5:68688–99.
3. Singhvi M, Gokhale D. Biomass to biodegradable polymer (PLA). RSC Adv. 2013;3:13558–68.
4. Papageorgiou GZ, Bikiaris DN. Crystallization and melting behavior of three biodegradable poly(alkylene succinates). A comparative study. Polymer. 2005;46:12081–92.

5. Ishii N, Inoue Y, Shimada K, Tezuka Y, Mitomo H, Kasuya K. Fungal degradation of poly(ethylene succinate). Polym Degrad Stab. 2007;94:44–52.
6. Lu J, Qiu Z, Yang W. Effects of blend composition and crystallization temperature on unique crystalline morphologies of miscible poly(ethylene succinate)/poly(ethylene oxide) blends. Macromolecules. 2008;41:141–8.
7. Woo EM, Hsieh Y, Chen W, Kuo N, Wang L. Immiscibility–miscibility phase transformation in blends of poly(ethylene succinate) with poly(L-lactic acid)s of different molecular weights. J Polym Sci Polym Phys. 2010;48:1135–47.
8. Tezuka Y, Ishii N, Kasuya K, Mitomo H. Degradation of poly(ethylene succinate) by mesophilic bacteria. Polym Degrad Stab. 2004;84:115–21.
9. Ueda AS, Chatani Y, Tadokoro H. Structure studies of polyesters. IV. Molecular and crystal structure of poly(ethylene succinate) and poly(ethylene oxalate). Polym J. 1971;2:387–94.
10. Gan Z, Abe H, Doi Y. Biodegradable poly(ethylene succinate)(PES). 2. Crystal morphology of melt-crystallized ultrathin film and its change after enzymatic degradation. Biomacromolecules. 2000;1:713–20.
11. Qiu Z, Ikehara T, Nishi T. Crystallization behavior of biodegradable poly(ethylene succiante) from the amorphous state. Polymer. 2003;44:5429–37.
12. Ichikawa Y, Washiyama J, Moteki Y, Noguchi K. Crystal modification in poly(ethylene succiante). Polymer. 1995;27:1264–6.
13. Zeng J, Zhu Q, Li Y, Qiu Z, Wang Y. Unique crystalline/crystalline polymer blends of poly(ethylene succinate) and poly(*p*-dioxanone): miscibility and crystallization behaviors. J Phys Chem B. 2010;114:14827–33.
14. Yang Y, Qiu Z. Crystallization and melting behavior of biodegradable poly(ethylene succinate-*co*-6 mol% butylene succinate). J Appl Polym Sci. 2011;122:105–11.
15. Li X, Qiu Z. Synthesis and properties of novel poly(ethylene succinate-*co*-decamethylene succinate) copolymers. RSC Adv. 2015;5:103713–21.
16. Li X, Qiu Z. Crystallization kinetics, morphology, and mechanical properties of novel poly(ethylene succinate-*co*-octamethylene succinate). Polym Test. 2015;48:125–32.
17. Wu H, Qiu Z. Synthesis, Crystallization kinetics and morphology of novel poly(ethylene succinate-*co*-ethylene adipate) copolymers. CrystEngComm. 2012;14:3586–95.
18. Qiu S, Su Z, Qiu Z. Crystallization kinetics, morphology and mechanical properties of novel biodegradable poly(ethylene succinate-*co*-ethylene suberate) copolyesters. Ind Eng Chem Res. 2016;55:10286–93.
19. Qiu S, Su Z, Qiu Z. Synthesis, thermal and mechanical properties and hydrolytic degradation of novel bio-based poly(ethylene succinate-*co*-ethylene sebacate) copolymers. (to be submitted for publication).
20. Liu T, Mo Z, Wang S, Zhang H. Nonisothermal melt and cold crystallization kinetics of poly(aryl ether ether ketone ketone). Polym Eng Sci. 1997;3:568–75.
21. Zeng J, Srinivansan M, Li S, Narayan R, Wang Y. Nonisothermal and isothermal cold crystallization behavior of biodegradable poly(*p*-dioxanone). Ind Eng Chem Res. 2011;50:4471–7.
22. Zhao Y, Qiu Z, Yan S, Yang W. Crystallization behavior of biodegradable poly(L-lactide)/multiwalled carbon nanotubes nanocomposites from the amorphous state. Polym Eng Sci. 2011;51:1564–73.
23. Yu J, Qiu Z. Isothermal and nonisothermal cold crystallization behaviors of biodegradable poly(L-lactide)/octavinyl-polyhedral oligomeric silsesquioxanes nanocomposites. Ind Eng Chem Res. 2011;50:12579–86.
24. Saad GR, Elsawy MA, Aziz MSA. Nonisothermal crystallization behavior and molecular dynamics of poly(lactic acid) plasticized with jojoba oil. J Therm Anal Calorim. 2016;. doi:10.1007/s10973-016-5910-z.
25. Henricks J, Boyum M, Zheng W. Crystallization kinetics and structure evolution of a polylactic acid during melt and cold crystallization. J Therm Anal Calorim. 2015;120:1765–74.
26. Shi N, Dou Q. Non-isothermal cold crystallization kinetics of poly(lactic acid)/poly(butylene adipate-*co*-terephthalate)/treated calcium carbonate composites. J Therm Anal Calorim. 2015;119:635–42.
27. Avrami M. Kinetics of phase change. II transformation-time relations for random distribution of nuclei. J Chem Phys. 1940;8:212–24.
28. Avrami M. Granulation, phase change, and microstructure kinetics of phase change. III. J Chem Phys. 1941;9:177–84.
29. Wunderlich B. Macromolecular physics, vol. 2. New York: Academic Press; 1976.
30. Zhang R, Zheng H, Lou X, Ma D. Crystallization characteristics of polypropylene and low ethylene content polypropylene copolymer with and without nucleating agents. J Appl Polym Sci. 1994;51:51–6.
31. Khanna Y. A barometer of crystallization rates of polymeric materials. Polym Eng Sci. 1990;30:1615–9.
32. Ozawa T. Kinetics of non-isothermal crystallization. Polymer. 1971;12:150–8.
33. Qiu Z, Fujinami S, Komura M, Nakajima K, Ikehara T, Nishi T. Nonisothermal crystallization kinetics of poly(butylene succinate) and poly(ethylene succinate). Polym J. 2004;36:642–6.
34. Qiu S, Qiu Z. Crystallization kinetics and morphology of poly (ethylene suberate). J Appl Polym Sci. 2016;133:43086.